FIGURE S1

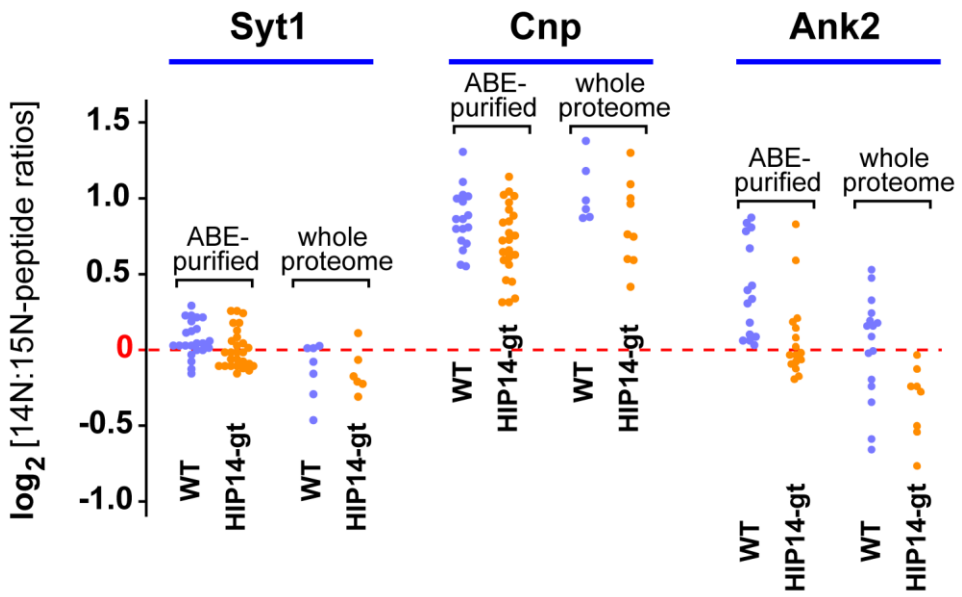

FIGURE S1. Comparison of peptide data scatter for ABE-purified and whole proteome samples (related to Figure 1). 14N/15N-ratios for peptides associated with three proteins, synaptotagmin 1 (Syt1), cyclic nucleotide phosphodiesterase (Cnp), and ankyrin 2 (Ank2), deriving from MS/MS runs of WT and *Hip14-gt* ABE/SILAM samples were compared with data from MS/MS analysis of minimally processed whole proteome SILAM samples. Syt1, Cnp, and Ank2 were chosen since these proteins show substantial representations in both the ABE-purified and the whole brain homogenate samples, thus allowing comparison. The whole proteome SILAM samples were prepared by a 1:1 mixing of crude brain homogenate from the 15N-reference mouse with homogenates from either a *Hip14-gt* mouse or its WT littermate.

FIGURE S2

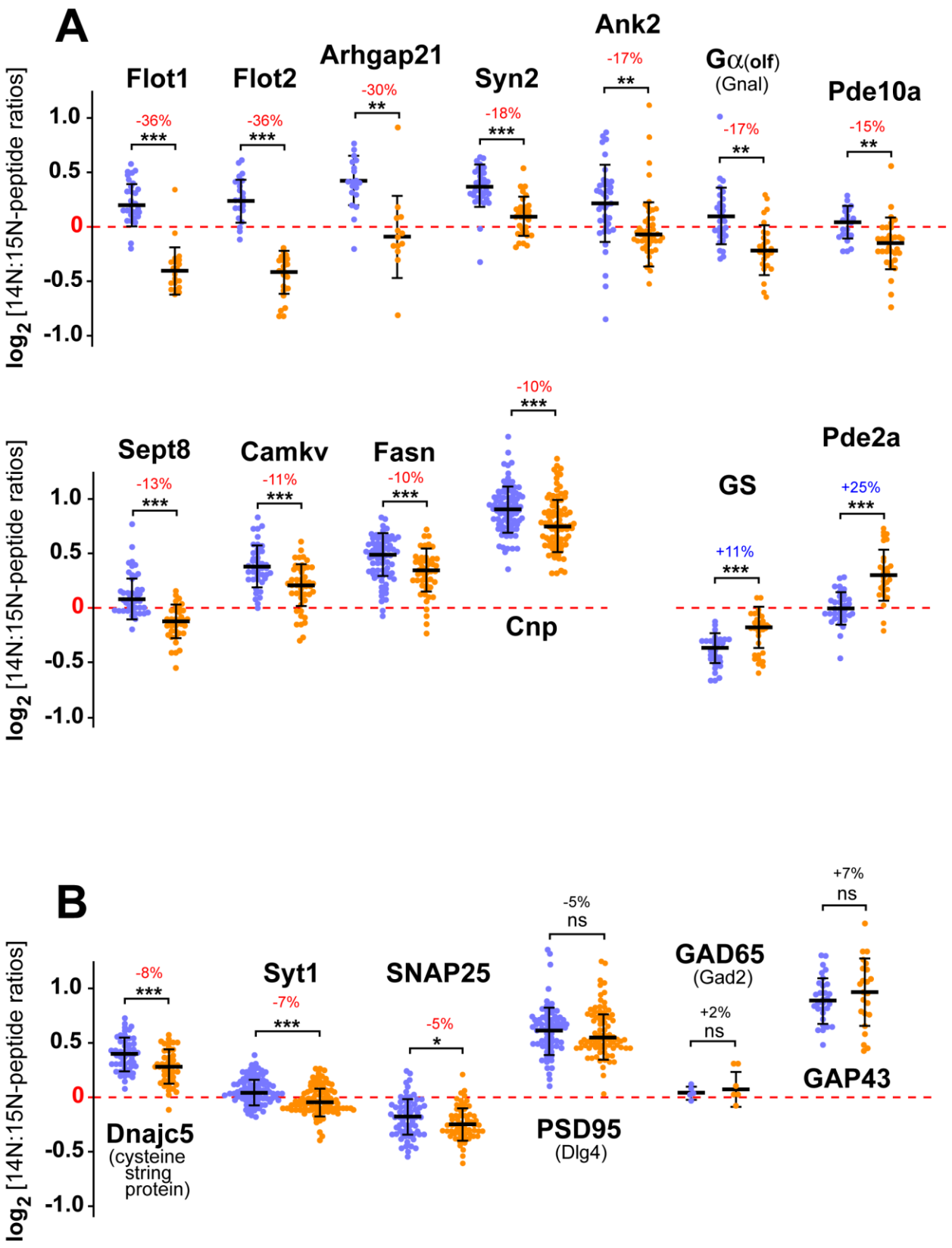

FIGURE S2. Graphical depiction of peptide data for selected palmitoyl-proteins from the *Hip14-gt* vs WT analysis (related to Tables 1 and 2). For the indicated proteins, $\log_2$ values of 14N/15N peak

volume ratios are reported for all peptides mapping. Data was aggregated both from four *Hip14-gt* mixed 14N/15N-ABE sample runs (HIP14-gt) and from the corresponding four WT littermate sample runs (WT). Median values +/- SD are shown, with the calculated change in *Hip14-gt* versus the WT littermate reported. Significance: *** P < 0.001, ** P < 0.01, * P < 0.05. (**A**) Peptide data for the thirteen proteins that show the most significant *Hip14-gt* change that are listed in Table 1. (**B**) Peptide data for six of the eight Table 2 proteins, identified by prior work as likely HIP14 palmitoylation substrates.

FIGURE S3

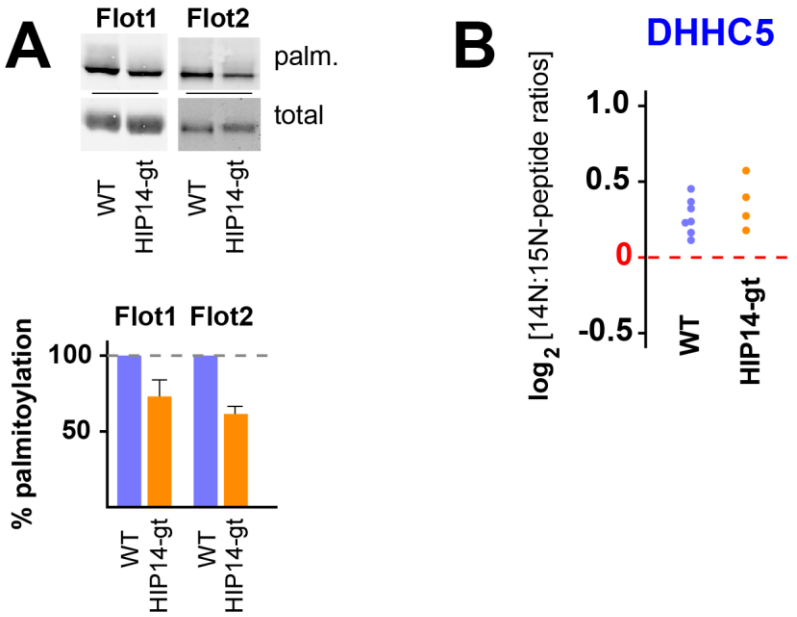

FIGURE S3. Comparison of *Hip14-gt* and WT littermate brain homogenates for Flot1 and Flot2 palmitoylation levels and for DHHC5 protein expression levels (related to Figure 2). (**A**) To analyze the effects of the *Hip14-gt* mutation on Flot1 and Flot2 palmitoylation, the two proteins were immunoprecipitated from whole brain homogenates of *Hip14-gt* and WT littermate animals and then subjected to ABE chemistry as described (Drisdel and Green, 2004). Biotinylated proteins were then blotted either with streptavidin-HRP to assess the extent of biotin replacement and hence palmitoylation (palm.) or with Flot1- or Flot2-specific antibodies (total). Example immunoblots are shown above, with quantification shown below. For the quantification (n = 2), biotin signals were normalized to the amount of signal derived from antibody detection of the total flotillin protein recovered from the immune precipitation. Thus, the reduced palmitoylation seen in *Hip14-gt* brain indicate reduced palmitoylation per protein. Data are presented as means +/- SEM. (**B**) Similar levels of palmitoylated DHHC5 in *Hip14-gt* and WT brain. Aggregated peptide datapoints from the four ABE/SILAM runs of the *Hip14-gt* and WT samples are reported. We interpret the similar ABE purification levels of DHHC5 in WT and *Hip14-gt* brain as an indication that there are similar levels of DHHC5 PAT activity in the two brains, as DHHC PAT auto-palmitoylation is well correlated with PAT activity (Lobo et al., 2002; Roth et al., 2002), presumably a reflection of the intermediary transfer of the acyl moiety to the enzyme prior to its transfer to substrate (Jennings and Linder, 2012; Mitchell et al., 2010).

FIGURE S4

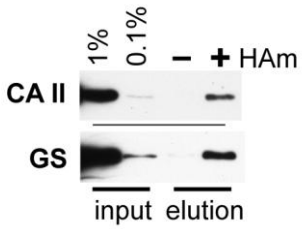

FIGURE S4. Low palmitoylation stoichiometries for CA II and GS in WT whole brain homogenate (related to Figure 4B). Complementing the Fig. 4B analysis, the portion of the input CA II and GS recoverable from thiol-Sepharose following acyl-RAC analysis was analyzed. The protein eluting from the thiol-Sepharose, following binding both in presence (+) and absence (-) of hydroxylamine (HAm), along with dilutions of the input homogenate were analyzed by immunoblot with antibody specific to either CA II or GS.

Legends for Supplemental Tables

Table S1: ABE/SILAM Data Summary for the Abundant Palmitoyl-Protein Set from the HIP14-gt/WT Analysis (supporting data for Tables 1 and 2)**.**

Data aggregated from the eight MS/MS runs comprising the *Hip14-gt* analysis is reported for the set of abundant palmitoyl-proteins, identified by an average of five or more peptides per run. Listed proteins are sorted by "HIP14/WT protein ratio" (see Supplemental Experimental Procedures). Proteins that showed >10% change (reduction or increase) in Hip14-gt relative to WT were subjected to an additional peptide level analysis. For this subset of proteins, some parameters of this peptide level analysis are additionally reported, including the total number of quantifiable peptides comprising the aggregated *Hip14-gt* and WT datasets ("# of peptides, Hip14-gt" and "# of peptides, WT"), the peptide-level ratio (the median *Hip14-gt* peptide value divided by the median WT peptide value; "Hip14/WT peptide ratios"), and the P-values from a Student's t-test comparison of each Hip14-gt and WT peptide dataset [significance thresholds: P < 0.05 (*), < 0.01 (**), and < 0.001 (***)]. The thirteen proteins identified as showing significant change of >10% their gene symbol highlighted either yellow (P < 0.01) or tan (P < 0.05). Several proteins were excluded due to extreme mouse-to-mouse 14N/15N-peptide datapoint variation between isogenic mice (highlighted pink).

The rightmost columns ("Palmitoylation Evidence from Prior Proteomic Analyses") summarize evidence, gleaned from prior palmitoyl-proteomic analyses that support (or do not support) palmitoylation for the proteins within our abundant palmitoyl-protein set. In ABE analysis, bonafide palmitoyl-proteins are typically distinguished from co-purifying, non-palmitoylated, contaminant proteins by assessing the relative hydroxylamine (HAm)-dependence of their purification (Kang et al., 2008; Roth et al., 2006), accomplished through the analysis of parallel, plus and minus-HAm samples, with the proteins that purify differentially into the plus-HAm samples being considered to be palmitoylated. Thus, data from our prior neural ABE analyses, which include parallel plus- and minus-HAm sample analyses, are also included ("Spectral Count Data: Plus/Minus HAm Ratios"); included are an analysis of mouse brain palmitoylation, as well as a published analyses of rat whole brain and neuronal culture palmitoylation (Kang et al., 2008). Data from these three analyses is reported as plus/minus-HAm spectral count ratios. High plus/minus ratios (e.g. >>1) indicate HAm-dependent purification and thus, likely palmitoylation. In addition, we also include relevant data, extracted from other published palmitoyl-proteomic reports. These reports utilized a variety of different cell types, with palmitoyl-proteomes being purified either by ABE-based methods or by click chemistry-based methods. This compilation was greatly faciliated by a prior compilation from Hang and colleagues (Wilson et al., 2011), which compared their results to results from other published reports (Kang et al., 2008; Martin and Cravatt, 2009; Yang et al., 2010; Zhang et al., 2008). In addition to this data, here we have also add in the data from two recent reports (Li et al., 2012; Marin et al., 2012). The likely palmitoyl-

proteins identified by these reports are dually designated with a plus symbol and with blue highlighting. In instances where the cited study identified a protein paralogous to the protein on our list (but not the actual listed protein), the paralogous protein is listed.

Table S2: ABE/SILAM Data Summary for the Abundant Palmitoyl-Protein Set from the YAC128/WT Analysis (supporting data for Table 3).

Data aggregated from the YAC128 ABE/SILAM analysis is reported for the abundant palmitoyl-protein set, these being proteins identified by an average of three or more peptides per run. Listed proteins are sorted by "YAC128/WT protein ratio" (see Supplemental Experimental Procedures). See Table S1 legend for explanation of the reported data categories.

SUPPLEMENTAL EXPERIMENTAL PROCEDURES

Mice

Hip14-gt, YAC128, and WT littermate mice were humanely housed and fed with standard mouse chow. *Hip14-gt* and YAC128 mice have been previously described (Singaraja et al., 2011; Slow et al., 2003). The WT littermate controls are the WT siblings of the transgenic models. Whole brain from YAC128 and WT littermates was harvested at 12 months of age, flash frozen in liquid nitrogen, then overnight shipped on dry ice, while brains from HIP14-gt and their WT littermates were harvested at 3 months. To generate 15N-labeled mice, wild-type mice of the C57Bl/6 background were fed a post-weaned diet, in which the protein component consisted of pelletized 15N-labeled Spirulina ((McClatchy et al., 2007); Cambridge Isotope Laboratories). Following 10 weeks on this restricted diet, whole brain was harvested, flash frozen in liquid nitrogen, then overnight shipped on dry ice. The Acyl-RAC-based analysis of palmitoylation stoichiometry, described below, utilized brain homogenates from 3 month-old C3H x C57Bl/6 f1 hybrid mice.

ABE/SILAM – Homogenate preparation and ABE purification

Whole frozen mouse brains were individually homogenized as previously described (Kang et al., 2008), each in 4 ml of cold Lysis Buffer (LB: 150 mM NaCl, 50 mM Tris, 5 mM EDTA, pH 7.4) with 10 mM N-ethylmaleimide (NEM) and 1x protease inhibitors (1xPI: 1 mM PMSF plus 2.5 μg/ml each of pepstatin, antipain, chymostatin, and leupeptin). The protein concentration of each homogenate was assessed by a modified Lowry assay (Lowry et al., 1951), which included 0.2% SDS in all samples and standards. Homogenates were stored at -80^{o}C for several weeks, prior to ABE sample purification. At the outset of the ABE palmitoyl-protein purification, equal 3.7 mg protein portions of the 14N-test and 15N-reference brain homogenates, which corresponds to approximately 10% of a homogenate, from an individual mouse brain, are first mixed together. The subsequent ABE palmitoyl-proteome purification followed the detailed published protocol (Wan et al., 2007), except for two modifications. The first modification involved the addition of a disulfide reduction step. Following the Triton X-100 homogenate solubilization step and the subsequent chloroform-methanol precipitation, protein pellets were solubilized into 1 ml of SDS Buffer (SB: 2% SDS, 50 mM Tris, 5 mM EDTA, pH 7) containing 1xPI and 10 mM tris(2-carboxyethyl)phosphine (TCEP). Following 20 min at 37^{o}C, NEM was added to 10 mM and the incubation was continued at 4^{o}C for 16 h, with end-over-end rotation. The second protocol departure was in the subsequent NEM removal step, where repeated ultra-filtration steps were substituted for the three chloroform-methanol precipitations. For this, following the overnight incubation, the 1 ml sample was diluted to 15 ml with LB containing 0.1% SDS and then transferred to Amicon Ultra-15 Centrifugal Filter Units (10 KDa molecular weight cutoff; EMD Millipore, Billerica, MA), which was spun for 30 min at 4000 x g in a swinging bucket rotor at 10^{o}C. The ~250 μl remaining volume was re-diluted with 15 ml LB plus 0.1% SDS and re-centrifuged. Following two additional

reiterations, the final 250 μl was removed from the filtration unit and combined with two washes of the unit, a 250 μl 4% SDS, 50 mM Tris, 5 mM EDTA, 1xPI, pH 7.4 wash and then a 200 μl 2% SDS, 50 mM Tris, 5 mM EDTA, pH 7.4 wash. Subsequent steps, i.e. the HAm-mediated thioester cleavage, the biotinylation, and the streptavidin-agarose binding were performed as previously described (Wan et al., 2007).

MS and Data Analysis

The ABE-purified samples were reduced with TCEP, alkylated with iodoacetamide, then trypsinized overnight as described (Butko et al., 2013; Savas et al., 2012). The resulting peptides were then analyzed by MuDPIT (Link et al., 1999; Washburn et al., 2001) using a LTQ Orbitrap XL (Thermo Finnigan, Palo Alto, CA) as described (McClatchy et al., 2012), except that an 8-step peptide fractionation protocol was used. Tandem mass spectra were searched against a combined light (14N) and heavy (15N) versions of the EBI-IPI mouse protein database (EBI-IPI_mouse_01-01-09), using RawExtract 1.9.9 (McDonald et al., 2004) and ProLuCID (Xu et al., 2006) as described (Butko et al., 2013), except that for two differences: first,125.047 was used as the static cysteine modification, this being the product of the ABE thiol blockade; second, only peptides with single tryptic C termini were considered. Parallel searches of a decoy database containing reversed sequences of the mouse database proteins (Peng et al., 2003), indicated that the protein false discovery rates to be <2% per ABE/SILAM sample. The quantification of relative light and heavy peptide amounts relied upon Census (Park et al., 2008). For each identified tandem mass spectra, Census first constructs an ion chromatogram from the MS1 data. Then, the complementary heavy or light ion chromatogram is constructed by analyzing MS1 data within the m/z range calculated for the paired peptide. Linear regression analysis of heavy/light chromatogram pairs was then used to derive a 14N/15N-ratio for each peptide. An important Census filter that identifies and removes poor quality measurements is the closeness of fit calculation (i.e. correlation coefficient), applied to the heavy and light chromatogram pairs. Paired chromatograms showing poor fit, i.e. with correlation coefficient values (r^2) of <0.5, were discarded. Census also filters data by removing the outlier peptide ratios, from the sets of peptide-ratio datapoints associated with individual proteins. Finally, to correct for error potentially introduced at the initial homogenate mixing step, Census also was used to normalize the overall 14N/15N-peptide ratio for each sample run to a median value of one; this adjustment, which assumes the differences between the 14N- and 15N-proteomes to be small (when averaged over entire proteomes), substantially improves sample-to-sample reproducibility. [Census is freely available for individual use and evaluation through an Institutional Software Transfer Agreement (see http://fields.scripps.edu/census for details).]

The comparison of each protein's representation within the mutant palmitoyl-proteome (either *Hip14-gt* or YAC128) to its representation within the age-matched, isogenic wild-type palmitoyl-

proteome, is accomplished using a ratio of ratios approach. For this, a 14N/15N-protein ratio is first derived for each protein by averaging the associated 14N/15N-peptide ratios from single MuDPIT runs. Next, 14N/15N-protein ratios are averaged together from like runs (i.e. both technical and biological replicates) and these two averaged ratios from the aggregated mutant and from the aggregated wild-type runs are compared ratiometrically (i.e. ratio of ratios). The aggregated datasets, organized by proteins, are sorted by these second-level ratios so that the proteins associated with the most extreme change are clustered at the top or the bottom of the list. In our analyses, the proteins at these two extremes tended to be dominated by proteins with weak MS detection, with only one or two peptide detections in some runs and no detections in other runs. In many instances, we found that average ratios were being skewed by one or several outlier peptide ratios. To minimize this noise, associated with a low volume of peptide data, we refocused our analysis on the set of ~300 palmitoyl-proteins that are detected by an average of five or more quantifiable peptides per run. Within this set, the proteins showing >10% change in mutant versus wild-type palmitoyl-proteomes, as determined by the above protein-level analysis, were selected for an additional peptide-level analysis, which compiled and analyzed all the quantifiable peptides from like runs (technical and biological replicates). In addition, this peptide-level analysis also utilized more stringent filtering, using the closeness of fit parament, r^2 values of > 0.81 were required for chromatogram pairs. In this approach, each individual peptide-level quantification serves as a separate, independent measure of a protein's representation within the 14N-test versus the 15N-reference palmitoyl-proteome. From these sets of peptide measurements associated with each protein, median 14N/15N-ratios, together with standard deviations were calculated. Median ratios from the mutant and wild-type datasets were then compared via the ratio of ratios approach to yield a final estimation of change for each palmitoyl-protein in mutant versus wild-type brain. The significance of these changes was assessed using Student's t-test to compare the set of mutant peptide ratios to the wild-type set. Overall, the changes identified showed good mouse-to-mouse reproducibility among the cohorts of age-matched, isogenic mice (see Supplemental Figure 6 for examples).

Antibodies

Protein-specific antibodies were purchased for use in both the Western and Acyl-RAC analyses: rabbit polyclonal antibodies to CA II (Abcam; Cambridge, MA), GS (Santa Cruz Biotechnology, Inc.; Dallas, TX), Flot1 (Mab; BD Biosciences; San Jose, CA), Flot2 (Mab; BD Transduction Laboratories), and SNAP-25 (SMI 81 Mab; Covance; Princeton, NJ), as well as mouse monoclonal antibodies to PSD-95 and Gαs (clones K28/43 and 192/12, respectively, from UC Davis/NIH NeuroMab Facility; Davis, CA).

Western quantification

To assay individual proteins for expression level change, portions of the brain homogenates used for the ABE/SILAM analyses, also were analyzed by quantitative Western blotting. Blots were developed using the Pierce ECL chemilumenescent system (Thermo Fisher Scientific Inc; Waltham, MA) and imaged with a LAS-4000 (Fujifilm; Tokyo, Japan). NIH Image was used for band quantification of the resulting TIFF images. Results for each of the assessed proteins, were normalized to the amount of SNAP-25 detected per homogenate, which was assumed to have invariant expression between homogenates.

Analysis of Substrate Specificity in Yeast

Yeast expression plasmids. The analysis of PAT substrate specificity in yeast required the sub-cloning cDNAs for the tested mammalian PATs and substrates into appropriate yeast expression plasmids, the source cDNA being human HIP14 (NM_015336.2; (Singaraja et al., 2002)), mouse DHHC5 (NM_144887.4), rat SNAP-25 (NM_030991.3), mouse Flot1 (NM_008027.2), and human Flot2 (NM_004475.2). Sequences encoding a tripartite 3xHA/FLAG/6xHis epitope tag (Roth et al., 2002) were appended to the C-terminus of the five ORFs to enable both immunoprecipitation and immunoblot detection. Enabling robust translational initiation in yeast, the 20 bp immediately upstream of the yeast *YCK2* ORF were engineered to the equivalent location upstream of the mammalian sequences. To facilitate proper termination and polyadenylation, yeast sequences also were added downstream, with the ~810 bp sequence, immediately downstream of the yeast *AKR1* ORF being added downstream of the expressed mammalian ORF sequences. The regulatable *GAL1* promoter was used for test substrate expression, while expression of the two PATs relied on two strong constitutive promoters – a 678 bp upstream *TDH3* fragment (-690 to -13, relative to *TDH3* ORF) for HIP14 expression and a 643 bp upstream *ACT1* fragment (-662 to -20, relative to *ACT1* ORF) for DHHC5. The yeast shuttle vector backbones used for these PAT and substrate expression plasmids were the *LEU2* pRS315 and *URA3* pRS316 yeast shuttle vectors (Sikorski and Hieter, 1989), respectively, the different selectable markers supporting pairwise introductions of substrate and PAT plasmids into the *ura3-52, leu2, his3* yeast strain LRB759 (Panek et al., 1997).

Click-based detection of palmitoylation in yeast. For this analysis, palmitoylation was detected with a click-based protocol (Charron et al., 2009), adapted to yeast as previously described (Roth et al., 2011). Briefly, log-phase cultures of LRB759, co-transformed with pairs of PAT and substrate expression plasmids, growing in YP-Raf (1% yeast extract, 2% peptone, 2% raffinose), were induced for expression of the test substrate protein by the addition of galactose to 2%. One hour subsequent to this galactose induction, metabolic labeling was initiated with the addition of the alkyne-tagged palmitate analog, 17-octadecynoic acid (ODYA; Cayman Chemical Corp.; Ann Arbor, MI) to 25 μM. Following a 1 h labeling period, 10^8 cells were harvested, protein extracts were prepared, with the substrate and PAT proteins then being anti-FLAG immune precipitated (Roth et al., 2011). The purified

proteins were then click-reacted with Alexa Fluor 647 Azide (Life Technologies; Grand Island, NY), subjected to SDS polyacrylamide gel electrophoresis, with the gel then transferred to a nitrocellulose membrane, which was fluorographically analyzed using a VersaDoc MP 5000 imaging system (Bio-Rad Laboratories; Hercules, CA). Expression levels of these proteins were monitored by parallel anti-HA Western blot analysis of a second identical gel.

Acyl-RAC-Based Analysis of Palmitoylation Stoichiometry

A modified acyl-RAC protocol (Forrester et al., 2011) was used both to confirm key ABE/SILAM results and to examine fractional palmitoylation status for selected individual proteins. For this, protein from a 10 mg protein portion of whole brain homogenate, prepared as for the above proteomic analysis in 1 ml of LB, containing 10 mM NEM and 1xPI protease inhibitors (1xPI: 1 mM PMSF plus 2.5 ug/ml each of pepstatin, leupeptin, antipain, and chymostatin), was collected by chloroform-methanol precipitation (Wan et al., 2007). The precipitated protein was dissolved into 0.5 ml of 4% SDS, 50 mM Tris, 10 mM NEM, 5 mM EDTA, pH7.4 for 10 min at 37^{o}C. Then, 0.5 ml of LB with 0.2% Triton X-100, 10 mM NEM and 1xPI was added and the sample was incubated for an additional 20 min at room temperature. NEM was then removed by ultrafiltration as described above, except that prior to the third and final iteration of the centrifugal ultrafiltration, Binding Buffer (BB: 100 mM HEPES, 1 mM EDTA, pH 7.4) with 0.1% SDS was used as the diluent. Finally, following the ultrafiltration, the concentrated 250 μl sample was transferred out of the filtration unit along with a 0.5 ml BB, 1% SDS wash of the unit. The thiol-blocked proteins were then absorbed to thiopropyl-Sepharose 6B (Sigma-Aldrich, St. Louis, MO) either in the presence or the absence of hydroxylamine. For this, 240 μl sample aliquots were mixed with either 80 μl of either 2 M hydroxylamine or with 0.8 M NaCl and then added to 30 μl of resin, pre-equilibrated with BB, containing 1% SDS. Following 4 h at 4^{o}C with rotation, unbound protein was removed and saved for further analysis, with the resin then being subjected to five 1-ml BB, 1% SDS washes. Finally, bound protein was eluted with 60 μl BB containing 1% SDS and 50 mM DTT in a 20 min, room temperature incubation. To assess the fraction of a particular protein that is palmitoylated, a portion of sample, saved prior to thiopropyl-Sepharose-6B binding, was compared via Western blotting to equivalent proportion of unbound sample, saved from both the plus- and minus-hydroxyamine bindings.

Data sharing. RAW files and complete parameter files will be publically available at http://fields.scripps.edu/published/ABE_SILAM upon publication.

SUPPLEMENTAL REFERENCES

Butko, M.T., Savas, J.N., Friedman, B., Delahunty, C., Ebner, F., Yates, J.R., 3rd, and Tsien, R.Y. (2013). In vivo quantitative proteomics of somatosensory cortical synapses shows which protein levels are modulated by sensory deprivation. Proc Natl Acad Sci U S A *110*, E726-735.

Charron, G., Zhang, M.M., Yount, J.S., Wilson, J., Raghavan, A.S., Shamir, E., and Hang, H.C. (2009). Robust fluorescent detection of protein fatty-acylation with chemical reporters. J Am Chem Soc *131*, 4967-4975.

Drisdel, R.C., and Green, W.N. (2004). Labeling and quantifying sites of protein palmitoylation. Biotechniques *36*, 276-285.

Forrester, M.T., Hess, D.T., Thompson, J.W., Hultman, R., Moseley, M.A., Stamler, J.S., and Casey, P.J. (2011). Site-specific analysis of protein S-acylation by resin-assisted capture. J Lipid Res *52*, 393-398.

Jennings, B.C., and Linder, M.E. (2012). DHHC protein S-acyltransferases use similar ping-pong kinetic mechanisms but display different acyl-CoA specificities. J Biol Chem *287*, 7236-7245.

Kang, R., Wan, J., Arstikaitis, P., Takahashi, H., Huang, K., Bailey, A.O., Thompson, J.X., Roth, A.F., Drisdel, R.C., Mastro, R., Green, W.N., Yates, J.R., 3rd, Davis, N.G., and El-Husseini, A. (2008). Neural palmitoyl-proteomics reveals dynamic synaptic palmitoylation. Nature *456*, 904-909.

Li, Y., Martin, B.R., Cravatt, B.F., and Hofmann, S.L. (2012). DHHC5 protein palmitoylates flotillin-2 and is rapidly degraded on induction of neuronal differentiation in cultured cells. J Biol Chem *287*, 523-530.

Link, A.J., Eng, J., Schieltz, D.M., Carmack, E., Mize, G.J., Morris, D.R., Garvik, B.M., and Yates, J.R., 3rd (1999). Direct analysis of protein complexes using mass spectrometry. Nat Biotechnol *17*, 676-682.

Lobo, S., Greentree, W.K., Linder, M.E., and Deschenes, R.J. (2002). Identification of a Ras palmitoyltransferase in Saccharomyces cerevisiae. J Biol Chem *277*, 41268-41273.

Lowry, O.H., Rosebrough, N.J., Farr, A.L., and Randall, R.J. (1951). Protein measurement with the Folin phenol reagent. J Biol Chem *193*, 265-275.

Marin, E.P., Derakhshan, B., Lam, T.T., Davalos, A., and Sessa, W.C. (2012). Endothelial cell palmitoylproteomic identifies novel lipid-modified targets and potential substrates for protein acyl transferases. Circulation research *110*, 1336-1344.

Martin, B.R., and Cravatt, B.F. (2009). Large-scale profiling of protein palmitoylation in mammalian cells. Nat Methods *6*, 135-138.

McClatchy, D.B., Dong, M.Q., Wu, C.C., Venable, J.D., and Yates, J.R., 3rd (2007). 15N metabolic labeling of mammalian tissue with slow protein turnover. J Proteome Res *6*, 2005-2010.

McClatchy, D.B., Liao, L., Lee, J.H., Park, S.K., and Yates, J.R., 3rd (2012). Dynamics of subcellular proteomes during brain development. J Proteome Res *11*, 2467-2479.

McDonald, W.H., Tabb, D.L., Sadygov, R.G., MacCoss, M.J., Venable, J., Graumann, J., Johnson, J.R., Cociorva, D., and Yates, J.R., 3rd (2004). MS1, MS2, and SQT-three unified, compact, and easily parsed file formats for the storage of shotgun proteomic spectra and identifications. Rapid Commun Mass Spectrom *18*, 2162-2168.

Mitchell, D.A., Mitchell, G., Ling, Y., Budde, C., and Deschenes, R.J. (2010). Mutational analysis of Saccharomyces cerevisiae Erf2 reveals a two-step reaction mechanism for protein palmitoylation by DHHC enzymes. J Biol Chem *285*, 38104-38114.

Panek, H.R., Stepp, J.D., Engle, H.M., Marks, K.M., Tan, P.K., Lemmon, S.K., and Robinson, L.C. (1997). Suppressors of YCK-encoded yeast casein kinase 1 deficiency define the four subunits of a novel clathrin AP-like complex. Embo J *16*, 4194-4204.

Park, S.K., Venable, J.D., Xu, T., and Yates, J.R., 3rd (2008). A quantitative analysis software tool for mass spectrometry-based proteomics. Nat Methods *5*, 319-322.

Peng, J., Elias, J.E., Thoreen, C.C., Licklider, L.J., and Gygi, S.P. (2003). Evaluation of multidimensional chromatography coupled with tandem mass spectrometry (LC/LC-MS/MS) for large-scale protein analysis: the yeast proteome. J Proteome Res *2*, 43-50.

Roth, A.F., Feng, Y., Chen, L., and Davis, N.G. (2002). The yeast DHHC cysteine-rich domain protein Akr1p is a palmitoyl transferase. J Cell Biol *159*, 23-28.

Roth, A.F., Papanayotou, I., and Davis, N.G. (2011). The yeast kinase Yck2 has a tripartite palmitoylation signal. Mol Biol Cell *22*, 2702-2715.

Roth, A.F., Wan, J., Bailey, A.O., Sun, B., Kuchar, J.A., Green, W.N., Phinney, B.S., Yates, J.R., 3rd, and Davis, N.G. (2006). Global analysis of protein palmitoylation in yeast. Cell *125*, 1003-1013.

Savas, J.N., Toyama, B.H., Xu, T., Yates, J.R., 3rd, and Hetzer, M.W. (2012). Extremely long-lived nuclear pore proteins in the rat brain. Science *335*, 942.

Sikorski, R.S., and Hieter, P. (1989). A system of shuttle vectors and yeast host strains designed for efficient manipulation of DNA in Saccharomyces cerevisiae. Genetics *122*, 19-27.

Singaraja, R.R., Hadano, S., Metzler, M., Givan, S., Wellington, C.L., Warby, S., Yanai, A., Gutekunst, C.A., Leavitt, B.R., Yi, H., Fichter, K., Gan, L., McCutcheon, K., Chopra, V., Michel, J., Hersch, S.M., Ikeda, J.E., and Hayden, M.R. (2002). HIP14, a novel ankyrin domain-containing protein, links huntingtin to intracellular trafficking and endocytosis. Hum Mol Genet *11*, 2815-2828.

Singaraja, R.R., Huang, K., Sanders, S.S., Milnerwood, A.J., Hines, R., Lerch, J.P., Franciosi, S., Drisdel, R.C., Vaid, K., Young, F.B., Doty, C., Wan, J., Bissada, N., Henkelman, R.M., Green, W.N., Davis, N.G., Raymond, L.A., and Hayden, M.R. (2011). Altered palmitoylation and neuropathological deficits in mice lacking HIP14. Hum Mol Genet *20*, 3899-3909.

Slow, E.J., van Raamsdonk, J., Rogers, D., Coleman, S.H., Graham, R.K., Deng, Y., Oh, R., Bissada, N., Hossain, S.M., Yang, Y.Z., Li, X.J., Simpson, E.M., Gutekunst, C.A., Leavitt, B.R., and Hayden, M.R. (2003). Selective striatal neuronal loss in a YAC128 mouse model of Huntington disease. Hum Mol Genet *12*, 1555-1567.

Wan, J., Roth, A.F., Bailey, A.O., and Davis, N.G. (2007). Palmitoylated proteins: purification and identification. Nature protocols *2*, 1573-1584.

Washburn, M.P., Wolters, D., and Yates, J.R., 3rd (2001). Large-scale analysis of the yeast proteome by multidimensional protein identification technology. Nat Biotechnol *19*, 242-247.

Wilson, J.P., Raghavan, A.S., Yang, Y.Y., Charron, G., and Hang, H.C. (2011). Proteomic analysis of fatty-acylated proteins in mammalian cells with chemical reporters reveals S-acylation of histone H3 variants. Mol Cell Proteomics *10*, M110 001198.

Xu, T., Venable, J.D., Kyu Park, S., Cociorva, D., Lu, B., Liao, L., Wohlschlegel, J., Hewel, J., and Yates, J.R., 3rd (2006). ProLuCID, a fast and sensitive tandem mass spectra-based protein identification program. Mol Cell Proteomics *5*, S174.

Yang, W., Di Vizio, D., Kirchner, M., Steen, H., and Freeman, M.R. (2010). Proteome scale characterization of human S-acylated proteins in lipid raft-enriched and non-raft membranes. Mol Cell Proteomics *9*, 54-70.

Zhang, J., Planey, S.L., Ceballos, C., Stevens, S.M., Jr., Keay, S.K., and Zacharias, D.A. (2008). Identification of CKAP4/p63 as a major substrate of the palmitoyl acyltransferase DHHC2, a putative tumor suppressor, using a novel proteomics method. Mol Cell Proteomics *7*, 1378-1388.